Magnetic Resonance in Medicine 64:939–946 (2010)

Diffusion-Weighted Spectroscopy: A Novel Approach to Determine Macromolecule Resonances in Short-Echo Time ^{1}H-MRS

N. Kunz,[1,2] C. Cudalbu,[1] V. Mlynarik,[1] P. S. Hüppi,[2] S. V. Sizonenko,[2] and R. Gruetter[1,3,4]*

Quantification of short-echo time proton magnetic resonance spectroscopy results in >18 metabolite concentrations (neurochemical profile). Their quantification accuracy depends on the assessment of the contribution of macromolecule (MM) resonances, previously experimentally achieved by exploiting the several fold difference in T_1. To minimize effects of heterogeneities in metabolites T_1, the aim of the study was to assess MM signal contributions by combining inversion recovery (IR) and diffusion-weighted proton spectroscopy at high-magnetic field (14.1 T) and short echo time (=8 msec) in the rat brain. IR combined with diffusion weighting experiments (with δ/Δ = 1.5/200 msec and *b*-value = 11.8 msec/μm^2) showed that the metabolite nulled spectrum (inversion time = 740 msec) was affected by residuals attributed to creatine, inositol, taurine, choline, *N*-acetylaspartate as well as glutamine and glutamate. While the metabolite residuals were significantly attenuated by 50%, the MM signals were almost not affected (<8%). The combination of metabolite-nulled IR spectra with diffusion weighting allows a specific characterization of MM resonances with minimal metabolite signal contributions and is expected to lead to a more precise quantification of the neurochemical profile. Magn Reson Med 64:939–946, 2010. © 2010 Wiley-Liss, Inc.

Key words: proton magnetic resonance spectroscopy; macromolecules; ultra-high field of 14.1 T; LCModel; quantification accuracy

INTRODUCTION

In vivo short echo time (TE) proton magnetic resonance spectroscopy (^{1}H-MRS) at high-magnetic field benefits from increased signal-to-noise ratio (SNR) and spectral dispersion, which improve quantification accuracy and precision, resulting in the direct measurement of the concentrations of about 18 metabolites (composing the neurochemical profile) in the rodent brain (1).

The accuracy of the quantification of the neurochemical profile is critically dependent on the estimation of the contribution of macromolecule (MM) resonances to the spectrum, overlapping with the metabolite's resonances. Therefore, an accurate assessment of the MM contribution is important since a biased estimation of the MM can lead to errors in the obtained metabolite concentrations (1,2). Since the MM resonances linewidth, in contrast to that of metabolites, does not increase substantially with B_0, it renders the distinction of MM signals from those of coupled spin systems more difficult. Furthermore, the absolute quantification of the MM concentrations may provide relevant information as a disease marker (3,4).

Different techniques to estimate the MM signals have been developed during the past years. When treating the MM as a mathematical unknown, a least-square fit using a sum of splines, wavelets, sinusoids, or polynomials with adjustable parameters to approximate the MM signals have been used (5–11). The MM baseline has also been assessed in a mathematical preprocessing step by modeling of the MM signals in the frequency domain with wavelets (1,7) or in the time-domain using singular value decomposition (2,4) and subsequent subtraction; truncation of initial data points (8,9); and "subtract" (5) or numerical filter approach (10). However, all the methods based on such mathematical modeling provide only an approximation of the true in vivo MM spectra (10–12). Although such mathematical approaches may allow a reasonably reliable estimation of the in vivo MM spectra at high-magnetic fields, where the MM spectrum includes relatively narrow resonances, additional prior knowledge is necessary for an accurate estimation of brain metabolite concentrations.

Therefore, to provide the necessary prior knowledge, an experimental assessment of the MM contributions, based on the separate acquisition of the in vivo MM spectra using the inversion recovery (IR) method (metabolite-nulled spectrum) has been used (13). However, using this experimental approach, small metabolite residuals are still present in the metabolite-nulled spectra due to variability in the T_1 relaxation times of metabolites (1,14). The identification of these metabolite residuals is mainly based on knowledge of the metabolites T_1 relaxation times and the consequent removal has been based on postprocessing techniques. Such a postprocessed in vivo MM spectrum was either added to the

[1]Laboratory of Functional and Metabolic Imaging (LIFMET), Ecole Polytechnique Fédérale de Lausanne, Lausanne, Switzerland.

[2]Division of Child Growth and Development, Department of Pediatrics, University of Geneva, Geneva, Switzerland.

[3]Department of Radiology, University of Geneva, Geneva, Switzerland.

[4]Department of Radiology, University of Lausanne, Lausanne, Switzerland.

Grant sponsor: SNSF; Grant numbers: 31003A-112233, 3100-067164, 405040-108713; Grant sponsor: EU Grant; Grant number: MRTN-CT-2006-035801; Grant sponsors: Centre d'Imagerie BioMedicale (CIBM) (of the UNIL, UNIGE, HUG, CHUV, EPFL), Leenaards and Jeantet Foundations.

*Correspondence to: R. Gruetter, Ecole Polytechnique Fédérale de Lausanne, SB - IPMC - LIFMET, Station 6, 1015 Lausanne, Switzerland. E-mail: rolf.gruetter@epfl.ch

Received 4 September 2009; revised 9 March 2010; accepted 31 March 2010.

DOI 10.1002/mrm.22490

Published online 17 June 2010 in Wiley Online Library (wileyonlinelibrary.com).

basis-set (15–19) during the quantification procedure or subtracted from the in vivo signal (11,20,21).

As described previously (1), MMs differ from metabolites by their T_1, which are ascribed to their larger molecular size. Consequently, the MM mobility as well as their diffusivity is more hindered. A previous study (22) has shown than MM have an apparent diffusion coefficient (ADC) 10–20 times lower than that of metabolites. Therefore, the use of diffusion weighting techniques could improve the MM baseline estimation by attenuating the metabolites signal without altering that of MM's.

Therefore, the aim of this study was to determine MM resonances without any postprocessing by combining metabolite-nulled spectra with diffusion weighting.

MATERIALS AND METHODS

Animals

In vivo experiments were performed on adult Sprague–Dawley (Charles-Rivers, France) rats ($n = 5$, ~350 g). The animals were anesthetized with a mixture of pure oxygen with 1.5–2% isoflurane administrated through a nose cone mask. Animals were restrained with a home-made holder with ear and tooth bars. Body temperature was measured by a rectal thermosensor and maintained at 37.5 ± 1°C by circulating warm water. Respiration and body temperature were monitored during the whole experiment by a small-animal monitor (SA Instruments, Inc., New York, NY). Animals were sacrificed at the end of the experience. All animal experiments were conducted according to federal and local ethical guidelines and the protocols were approved by the local regulatory body.

Instruments and Pulse Sequences

All in vivo experiments were performed on a Varian INOVA console (Varian, Palo Alto, CA) connected to a 14.1 T magnet with a 26-cm horizontal bore (Magnex Scientific, Abingdon, UK), and with an actively shielded gradient coil allowing a maximum gradient of 400 mT/m with a fix rise time of 120 μsec. A home-built quadrature surface coil consisting of two geometrically decoupled single loops of 14 mm of diameter was used as a transceiver.

Fast-spin echo images (repetition time [TR]/TE = 6000/72 msec, echo-train length = 16, field of view = 23 mm × 23 mm, acquisition matrix = 256 × 256, slice thickness = 0.8 mm, six averages) were acquired in 12 min to position the voxel for spectroscopy. Localized spectroscopy was performed on a typical volume of interest (VOI) of 140 μL with a short-echo time STEAM sequence (TE/mixing time [TM]/TR = 8/200/2500) with asymmetric radio frequency pulses for slice selection (1). The outer volume signal was suppressed by four blocks of slice selective pulses interleaved with the VAPOR scheme for water signal suppression, as described previously (1). Field homogeneity was adjusted by the correction of the first- and second-order shims using the echo planar version of FASTMAP (22).

The measurement of the in vivo MM spectrum was performed by adding an IR and a diffusion-weighted (DW) module to the STEAM sequence. IR was performed using a nonselective full-passage hyperbolic secant RF pulse (pulse length = 4 msec, bandwidth = 5 kHz) at different inversion times (TIs, ranging from 520 to 1000 msec). For the DW module, gradients were added in the TE/2 periods and applied simultaneously along the three gradient directions [1, 1, 1] (22) with a $\delta/\Delta = 1.5/200$ msec. The gradient strength ranged from 0 to 370 mT/m resulting in b-values ranging from 0 to 13.19 msec/μm^2. To compensate for magnetic field drift spectra were acquired in blocks of 16 averages, which were stored separately and were corrected for relative shift in frequency before summation.

To validate the DW-MRS protocols, the sequence was tested into two separate phantoms filled with water with a corrected pH of 7.4 and with respectively Cr and Glu, or NAA, Gln and Ins dissolve at a concentration of 30 mM. To assess the phase stability during acquisition, the spectra were acquired on a scan by scan basis for a total of 32 spectra for each b-values. The experience was performed for b-values up to 2 msec/μm^2. To investigate higher b-values, a set of in vivo data was also acquired for b-values up to 13.9 msec/μm^2. Each individual spectrum was analyzed by LCModel and the phase output was used to evaluate the experiments stability.

In addition to the in vivo MM spectra, in vivo brain spectra were acquired from five adult rats using the ultrashort TE spin echo full intensity acquired localization (SPECIAL) sequence (TE=2.8 msec) (23), which provides spectra with higher SNR than STEAM. The VOI was identical with that from where the MM spectra were acquired. Metabolite concentrations were estimated by LCModel. Quantification was performed using two different basis-sets composed of metabolite spectra simulated at TE = 2.8 msec, using a program written in MATLAB (MathWorks, Natick, MA) based on the density matrix formalism (24), using published values of coupling constants and chemical shifts (25). The results provided the quantification of the following metabolite concentrations: alanine (Ala), ascorbate (Asc), aspartate (Asp), creatine (Cr), γ-aminobuttyric acid (GABA), glucose (Glc), glutamate (Glu), glutamine (Gln), glutathione (GSH), glycerophosphorylcholine (GPC), phosphorylcholine (PCho), myo-inositol (Ins), lactate (Lac), *N*-acetylaspartate (NAA), *N*-acetylaspartylglutamate (NAAG), phosphocreatine (PCr), phosphoethanolamine (PE), scyllo-inositol (Scyllo), and taurine (Tau). To investigate the influence of the MM signals on the quantification results, a first basis-set contained the MM signals acquired in vivo at 2.8 msec with IR. Residual resonances at 3.9, 3.6, 3.4, 3.2, 2.7, and 2.0 ppm were removed by postprocessing as described previously using Hankel–Lanczos singular value decomposition (14). The second basis-set contained the MM signals acquired in this study using IR combined with diffusion weighting.

RESULTS

To determine the TI where most metabolite signals were minimized, IR measurements were performed at different TIs. As shown in Fig. 1, the cancellation of the metabolite signals occurred at different TI (e.g., Tau and NAA at 800 msec, Cr CH_2 group at 600 msec and several at 740

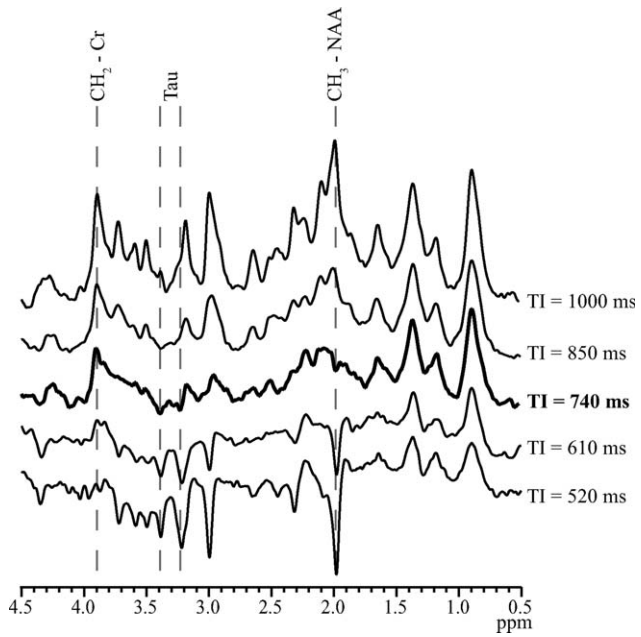

FIG. 1. Inversion recovery spectra acquired with STEAM (TE/TM/TR = 8/200/2500 msec, 256 averages) at TI = 520/610/740/850/1000 msec. A shifted gaussian filter ($\exp\left[-(t-0.06)^2/0.12^2\right]$) in combination with a light line broadening filter (exp[−5*t*]) were applied for modest resolution enhancement and noise reduction. Metabolite signal intensities vary with TI (inverted signal at TI = 520 msec and back to positive at TI = 1000 msec). The optimum metabolite-nulled spectrum was acquired at TI = 740 msec. However, contamination of *N*-acetylaspartate, creatine and taurine, and others are still present.

msec such as Glu, Gln, Ins, and more), which was ascribed to differences in T_1 (1,14). The MM signal, which has a T_1 = 300–600 msec (1), was almost completely recovered at the TIs used here. Except for the MM resonance at 0.9 ppm, which presumably comprises signals of methyl groups with increased mobility and correspondingly longer T_1 relaxation times, the variability of the spectral pattern in Fig. 1 can be assigned to changing peak intensities of metabolites.

The TI showing the smallest residuals of metabolites was 740 msec (Fig. 1). While a few narrow residuals assigned to metabolites were still discernible at 3.9 ppm, 3.4 ppm, 3.2 ppm, and at 2.01 ppm, the identification of incompletely nulled broader J-coupled resonances was less apparent, due to their apparent peak width approaching that of the MMs.

When applying IR at such determined near-optimal TI of 740 msec, together with diffusion weighting resulted in a progressive reduction of several spectral features in the metabolite-nulled spectrum (Fig. 3) with *b*-value increasing from 0 to 13.19 msec/μm^2. For example, resonances at 2.01, 3.2, 3.4, and 3.9 ppm are shown as dashed line in Fig. 3. These resonances are consistent with the presence of incompletely suppressed signals from creatine, taurine, *N*-acetylaspartate, and others.

To assess the stability of the diffusion weighting experiments, non-IR spectra were acquired with diffusion weighting on a scan by scan basis to investigate phase variation. At long diffusion time (Δ = 200 msec) and *b*-values up to 2 msec/μm^2 in phantom and from 0 to 13.9 msec/μm^2 in vivo, the phase stability was acceptable over the whole acquisition (cf. Fig. 2a,b). The makeable increase in the phase instability in the phantom at *b*-values = 1.9 and 2.5 msec/μm^2 was due to strong attenuation of the metabolites resonances in solution, which made their analysis by LCModel very uncertain.

To illustrate the negligible effect of diffusion weighting on MM signals, the spectrum without diffusion gradients was compared to DW spectrum (n = 4) with a *b*-value = 11.8 msec/μm^2. Direct subtraction of the two spectra was possible without applying amplitude correction and yielded a difference spectrum showing a near complete cancellation of the MM signals (top trace in Fig. 3). Overall, metabolite signals were attenuated by a factor 2 in the DW spectra, while the MM signal was affected by <8%. The difference spectra demonstrated an increased spectral dispersion at 14.1 T; such as the separation of GSH, NAA, and Gln resonances at 2.5 ppm (bottom trace in Fig. 3). The NAA resonance at 4.4 ppm is no more saturated by the water suppression at 14.1 T. In addition, the flat baseline after subtraction revealed metabolite resonances otherwise overlapped by MM signals, e.g., lactate (1.32 ppm and 4.1 ppm), alanine (1.47 ppm), or GABA (1.9 ppm) (Fig. 3).

Similar to the acquisition without IR (Fig. 3), MM signals in the IR experiments were minimally affected (<10% at b = 11.8 msec/μm^2) by the diffusion weighting (Fig. 4). Consequently, subtracting the DW spectra acquired at b = 11.8 msec/μm^2 with IR (TI = 750 msec) to the one acquired at b = 0 msec/μm^2, showed complete elimination of broad spectral features ascribed to MM, such as the 0.9, 1.2, and 1.4 ppm resonances (top trace in Fig. 4). Positive and negative signal differences were evident in the difference spectrum (top trace in Fig. 4). Positive residuals, consistent with a shorter T_1, were ascribed to glutamine/glutamate at 2.15 ppm, CH_2 group of *N*-acetylaspartate from 2.45 to 2.55 ppm, creatine at 3.9 ppm, choline at 3.2, myo-inositol at 3.55 ppm; and the negative signals, consistent with a longer T_1: CH_3 group of *N*-acetylaspartate at 2.01 ppm, and taurine at 3.4 and 3.25 ppm.

Figure 5 shows results of quantification (black bars) obtained using the MM spectrum acquired with IR combined with DW spectroscopy (STEAM, TE = 8 msec, *b*-value = 11.8 msec/μm^2) and, in gray bars, the quantification results obtained using the MM signal acquired with SPECIAL at 2.8 msec using IR and corrected by postprocessing. Overall, the two neurochemical profiles were in excellent agreement, though some metabolites showed a significant increase ~30% ($P < 0.05$, unpaired *t*-test) such as aspartate, glutamine, ascorbate, NAAG, and total choline when using the postprocessed MM basis.

To investigate the potential influence of the increased TE and TM on the measurement of the DW MM baseline, three IR spectra were acquired with STEAM (TI = 740 msec with (a) TE/TM = 2.8/20 msec, (b) 8/20 msec, and (c) 8/200 msec, cf. Fig. 6). From the two first traces, a reduction of 25% of the MM signals due to T_2 losses was noted. This is in excellent agreement with apparent T_2

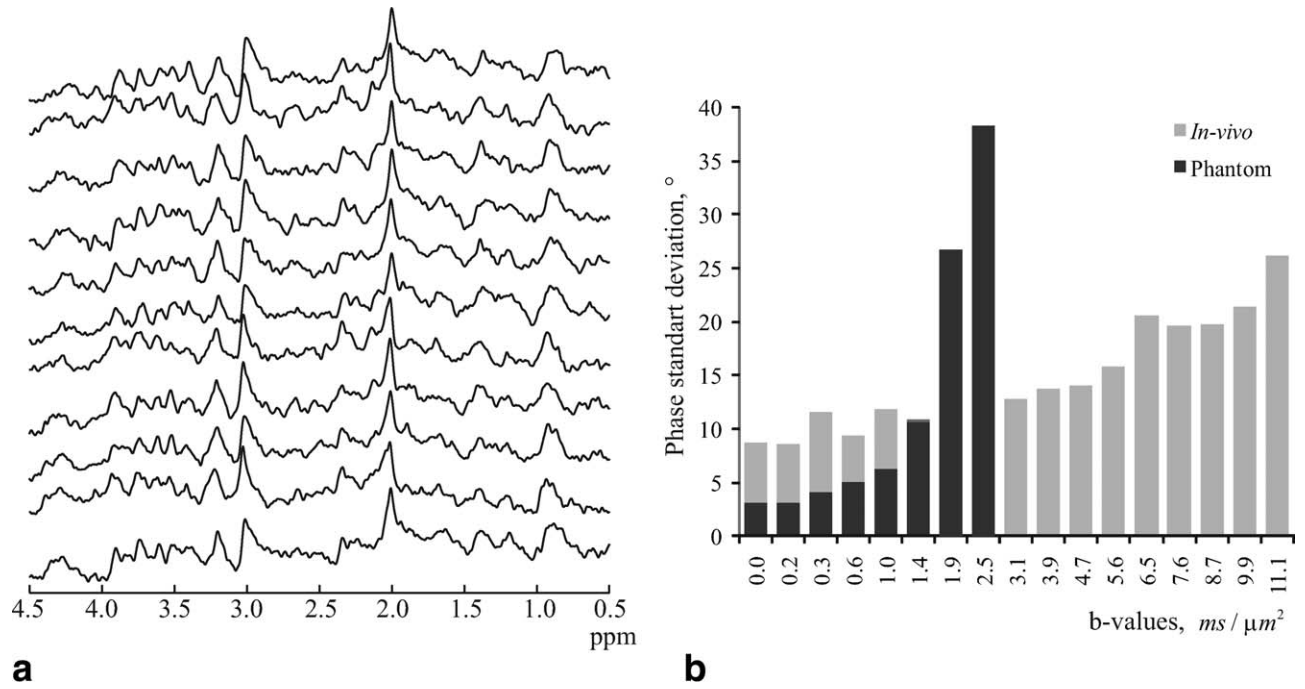

FIG. 2. **a**: Stack plot of individual in vivo ^{1}H-MRS scans acquired with STEAM (TE/TM/TR = 8/200/2500 msec and b = 11.8 msec/μm^2). A line broadening filter (exp[$-5t$]) was applied to reduce noise. No individual phase corrections were applied. Note a very stable phase during signal averaging. **b**: Phase standard deviation in function of b-value measured in phantom (dark gray) and in in vivo adult rat brain (light gray).

(19 ± 0.4 msec) values published at 9.4 T (26,27). However, the use of a long TM of 200 msec shows a significant attenuation due to T_1 relaxation. As for the T_2 effects, the T_1 attenuation seems to show very moderate fluctuations, resulting on an overall signal reduction without a strong shape modification.

DISCUSSION

This study demonstrates that the MM resonances can be identified in vivo with localized DW proton spectroscopy. The attenuation of 50% of the metabolite signals at b = 11.8 msec/μsec^2 was in good agreement with ADC values reported previously (22). Furthermore, the spectral quality of the DW spectra was excellent and comparable with the non-DW-spectra (Fig. 3).

To demonstrate the stability of the experiments, phantom studies were performed to b-values up to 2.5 msec/μm^2 due to the higher diffusivity of metabolites in water. Indeed, the ADC of metabolites was six times higher than in vivo (i.e., ~0.6 μm^2/msec in water vs. ~0.1 μm^2/msec in brain (28)). Therefore, in vivo experiments have been performed at higher b-values (0–13.9 msec/μm^2). The stack plot presented in Fig. 2a shows modest phase fluctuation, with a tendency to increase with the b-value. The MM signal attenuation measured at a b-value of 11.8 mm/μsec^2 was very low (<8%) and corresponds to an estimated ADC of ~0.007 μm^2/msec, which was in excellent agreement with the previously published value (22), suggesting a minimal influence of potential phase instabilities. The additional signal loss at high b-values due to the small phase instabilities would result in the same reduction of all signals in a spectrum, which should not alter the MM baseline and therefore should have a negligible impact on the conclusion of this study.

In parallel to the notable spectral quality and stability of the DW-experiments already discussed earlier, it is important to emphasize that the notable long diffusion time (Δ = 200 msec) and a short-gradient duration (δ = 1.5 msec) ensure a strong diffusion weighting (b-value up to 13.2 mm/μsec^2). In addition, the TM period of the STEAM-based sequence permitted the use of a relatively short TE of 8 msec with a long diffusion time, allowing the investigation of MM resonances (T_2 ~ 30 msec) using DW-MRS. On the other side, the SPECIAL sequence preserves the full intensity of the signal, increasing considerably the SNR and so decreasing the acquisition time. Therefore, for in vivo acquisition of the neurochemical profile, the SPECIAL sequence is more suitable. However, the design of the pulse sequence, based on a spin-echo scheme, does not allow sufficiently high b-value with a short TE to investigate the MM signals. Despite the different conception of the two sequences, SPECIAL and STEAM have quasi identical lineshape at such small TE (23). In addition, the ultrashort TE used during this study, insure minimal J-modulations or multiple quantum effects for both methods (i.e., SPECIAL with TE = 2.8 msec and STEAM with TE = 8 msec) (29). However, the long TM period, in the STEAM sequence, can affect the MM signal due to probable heterogeneities in MM T_1. Except for the MM resonances at 0.9 ppm, the MM T_1's were assumed to not be substantially different, resulting in a global attenuation of the MM baseline without altering the shape (cf. Fig. 6).

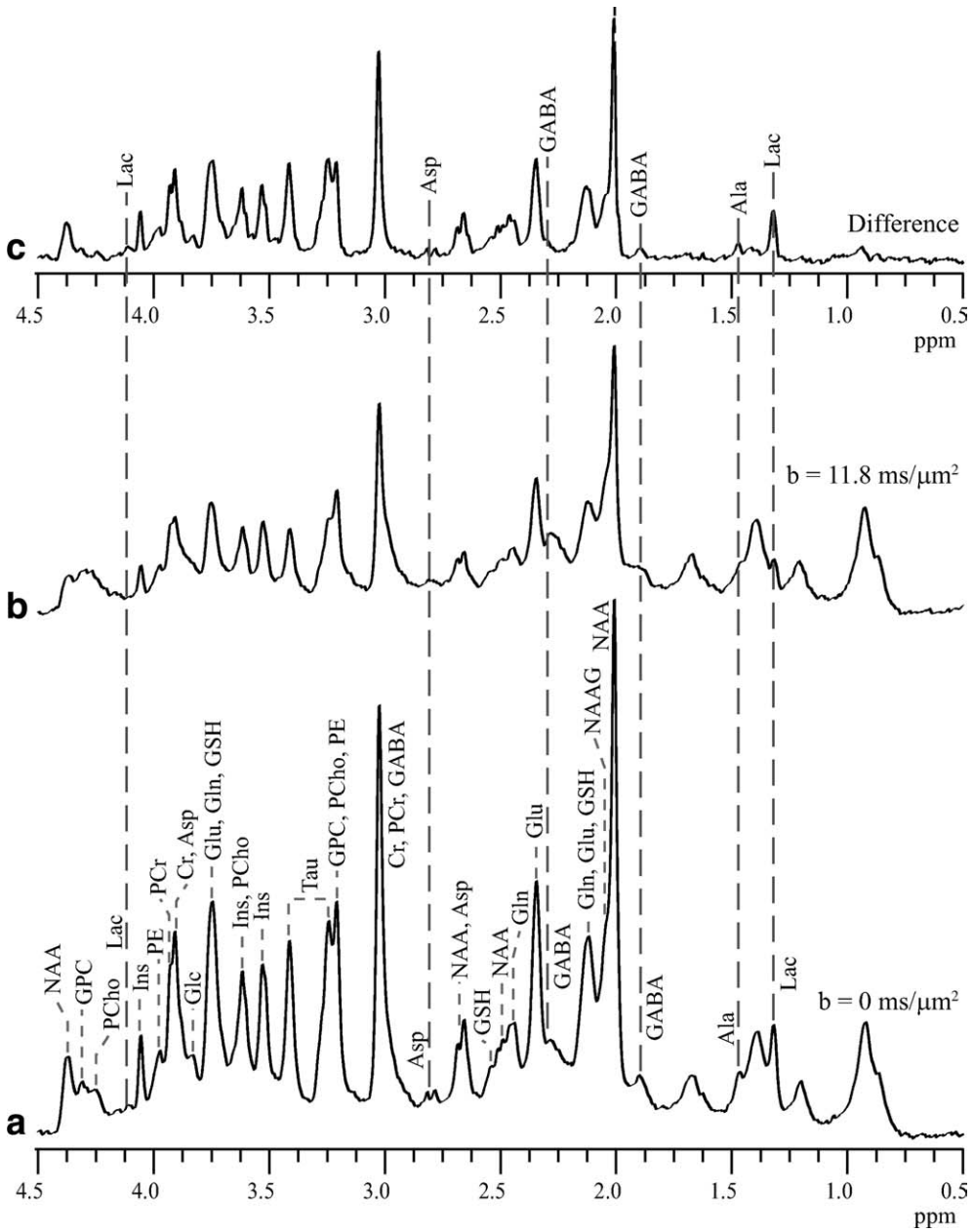

FIG. 3. ^{1}H-MRS spectra acquired with STEAM (TE/TM/TR = 8/200/2500 msec, 256 averages) (spectrum **a**) without diffusion gradient (b = 0 msec/μm^2) and (spectrum **b**) with diffusion gradient (b = 11.8 msec/μm^2). A shifted gaussian filter $\exp\left[-(t-0.06)^2/0.12^2\right]$ in combination with a light line broadening filter ($\exp[-5t]$) were applied for modest resolution enhancement and noise reduction. A difference spectra (spectrum **c**) was obtained after direct subtraction of peaks (**a**) and (**b**) without any amplitude correction (scaled up two times for display). Metabolites resonances in the lower part of the ppm scale (γ-aminobutyric acid (GABA), alanine (Ala), lactate (Lac), and aspartate (Asp)), which are strongly overlapped with macromolecules signals, are completely resolved in the difference spectra.

The heterogeneity of the metabolite T_1 relaxation times (Fig. 1) limits the IR technique to an incomplete nulling of the entire pool of metabolites (Fig. 4). Indeed, the presence of the residual of the CH_2 group of creatine at 3.9 ppm was already reported by Pfeuffer et al. (1) and others (30,31) as well as that of taurine at 3.2 and 3.4 ppm. Recently, Mlynárik et al. (14) reported that additional residuals from metabolites contribute to the metabolite-nulled spectrum such as choline at 3.2 ppm, NAA at 2 and 2.6 ppm and Ins 3.6 ppm, which have been removed by postprocessing (32). In this study, we confirmed the presence of these signal residuals, and so far uncovered additional residuals ascribed to glutamine and glutamate at 2.1 ppm (Fig. 4).

IR at TI = 740 msec led to near complete elimination of the metabolite signals (>80%, Fig. 1), but the remaining signals can still alter significantly the quantification (e.g. creatine, taurine and *N*-acetylaspartate). Postprocessing techniques can be used to remove the observable residual signals and thus to estimate the true MM signals. However, at high-magnetic field (>7 T), the estimation of the contaminating signals becomes increasingly difficult as the linewidth of J-coupled metabolites approach that of the MMs. Therefore, the lack of an accurate and complete identification of the residuals leads to incomplete nulling of the metabolite signals by postprocessing. In addition, even known small contributions of broad residuals, such as Cho and Ins, are probably difficult to remove by postprocessing, due to their large linewidth and small signal intensities.

Adding DW at a b-value = 11.8 mm/μsec^2 to the IR preparation attenuated 50% of the residual metabolite

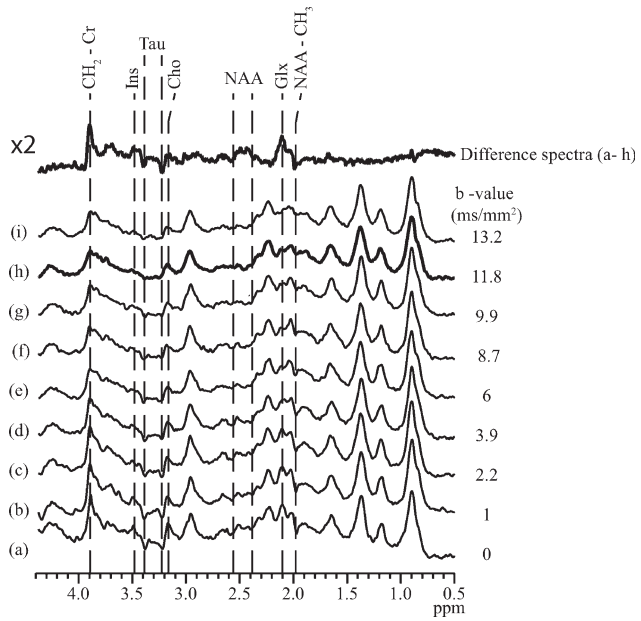

FIG. 4. Diffusion-weighted spectra combined with inversion recovery acquired with STEAM (TE/TM/TR = 8/200/2500 msec, TI = 740 msec, 720 averages). Diffusion gradient were gradually increased, giving *b*-value ranging from 0 (a) to 13.2 msec/μm^2 (i). The difference spectra between the $b = 0$ (a) and $b = 11.8$ msec/μm^2 (h) have a very flat baseline, demonstrating the insensitivity of macromolecules to diffusion weighting experiment. Additionally, several metabolite residuals can be identified in the difference spectra such as creatine (Cr), inositol (Ins), taurine (Tau), *N*-acetylaspartate (NAA), and glutamine and glutamate compounds (Glx).

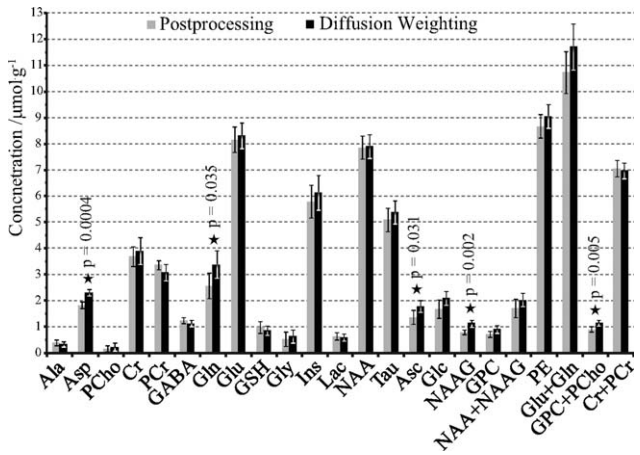

FIG. 5. Neurochemical profile of five adult rats acquired with SPECIAL (TE = 2.8 msec) assessed with LCModel (mean ± SD), using the DW-MM baseline (black, STEAM, TE = 8 msec) and the postprocessing MM baseline (gray, SPECIAL, TE = 2.8 msec). Few metabolites (*) show a significant increase aspartate (Asp), glutamine (Gln), ascorbate (Asc), and total choline (tCho) with a *P*-value <0.05 (unpaired *t*-test).

signals with slight attenuation on the MM resonances (<8%) compared with the *b*-value = 0 metabolite nulled spectra. Overall, it poised to a ~ 10-fold reduction of the metabolites signals (Fig. 4). Broader resonances overlapping with those of *N*-acetylaspartate, choline, glutamate, and glutamine were eliminated. It is thus likely that the final signal obtained is composed of the MM signals with negligible metabolite signals reduced to noise level.

The neurochemical profile assessed by LCModel using the MM signal determined with diffusion weighting overall agreed very well with the quantification performed with MM signal corrected by postprocessing (Fig. 5). Increasing the TE from 2 to 8 msec did not produce any relevant alteration on the MM signals (Fig. 6, peak b), except the general 5% attenuation due to T_2

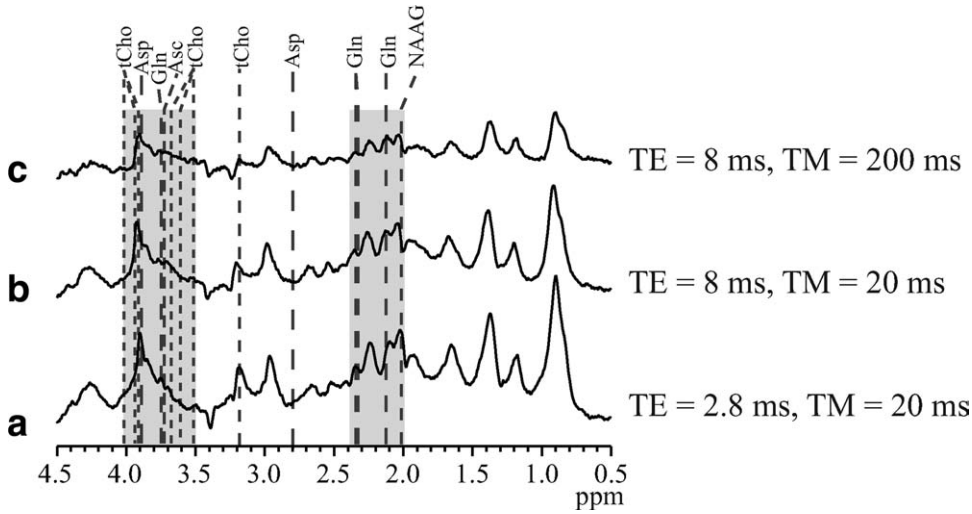

FIG. 6. IR-MRS with TI = 740 msec acquired with the STEAM sequence. (spectrum **a**) MM baseline with same TE = 2.8 msec and TM = 20 msec than for the quantification ^{1}H-MRS spectra. (spectrum **b**) The echo time was increased to TE = 8 msec with TM = 20 msec to investigate T_2 relaxation effects showing an overall reduction of ~25%. (spectrum **c**) To investigate the influence of the long TM a last MM baseline have been acquired with TE = 8 msec and TM = 200 msec. A significant signal dropped is visible due to T_1 relaxation. No strong modulation due to T_1 heterogeneities, which could alter quantification, has been noticed. ^{1}H-NMR resonances of aspartate, glutamine, ascorbate, and total choline are shown with the dashed lines.

relaxation. However, a significant loss of signal due to T_1 relaxation during the TM period of 200 msec has been noted (cf. Fig. 6, peak c). The attenuation looks rather homogenous, altering the absolute quantification of the MM signals. Indeed, the shape of the MM resonances, apart from a general scaling effect, show very little variations. Thus, the concentration increase of ~30% for some metabolites suggests incomplete metabolite nulling in the non-DW MM spectra. Indeed, all the metabolites showing an increase in concentration have ^{1}H-NMR resonances in one or both of the following frequency ranges: 2–2.4 ppm and 3.5–4 ppm (25). Comparing these two groups of resonances with the metabolite residuals removed with diffusion weighting, a good agreement with both spectral regions containing the most important metabolite residuals can be seen (top trace in Fig. 3). Thus, the increased concentrations of glutamine, aspartate, total choline, ascorbate, and *N*-acetylaspartylglutamate are likely due to a better elimination of these metabolite residuals by using the diffusion weighting technique.

The presented approach to assess the MM baseline, as all existing techniques, remains an approximation of the true baseline. In addition, the gap between the acquisition parameters of an optimal in vivo ^{1}H-MRS (e.g., TE = 2.8 msec and TM = 20 msec) and a DW-MRS sequences (e.g., TE = 8 msec, TM = 200 msec, and *b*-value > 10 mm/μsec^2), may add some imperfection in the quantification. However, the present technique improves the state-of-art by determining the MM signals purely experimentally, based on the larger molecular size of the MM proteins compared with metabolites, which results in a shorter T_1 and a smaller ADC. Therefore, IR combined with diffusion weighting probably leads to an accurate identification of the MM signals obviating eliminating the need for any postprocessing. It results in an excellent assessment of the MM baseline with residual contamination within the magnitude of the normal measurement variations.

We conclude that diffusion weighting combined with IR results in a direct and accurate approach to assess MM signals, which can be extended to any magnetic field. The proposed technique may be limited by system stability and subject motion, which for human systems would be very challenging due to stronger phase variation. However, the precise identification of the metabolites residuals present in the metabolite nulled spectra may provide relevant used as prior knowledge for postprocessing techniques.

REFERENCES

1. Pfeuffer J, Tkac I, Provencher SW, Gruetter R. Toward an in vivo neurochemical profile: quantification of 18 metabolites in short-echo-time (1)H NMR spectra of the rat brain. J Magn Reson 1999;141: 104–120.
2. Cudalbu C, Beuf O, Cavassila S. In vivo short echo time localized 1H MRS of the rat brain at 7 T: influence of two strategies of background-accommodation on the metabolite concentration estimation using QUEST. J Sign Process Syst 2008;55:25–34.
3. Hakumaki JM, Grohn OH, Pirttila TR, Kauppinen RA. Increased macromolecular resonances in the rat cerebral cortex during severe energy failure as detected by 1H nuclear magnetic resonance spectroscopy. Neurosci Lett 1996;212:151–154.
4. Ratiney H, Srinivasan R, Henry RG, Okuda D, Nelson S, Pelletier D. Early and progressive disease marker in MS: results from a large cross-sectional spectroscopic imaging study at 3T. In: American academy of neurology 59th annual meeting. Boston, MA; May 2007. p 02.041.
5. Lemmerling P, Vanhamme L, in't Zandt H, van Huffel S, van Hecke P. Time-domain quantification of short-echo-time in-vivo proton MRS. MAGMA 2002;15:178–179.
6. Provencher SW. Estimation of metabolite concentrations from localized in vivo proton NMR spectra. Magn Reson Med 1993;30:672–679.
7. Provencher SW. Automatic quantitation of localized in vivo 1H spectra with LCModel. NMR Biomed 2001;14:260–264.
8. Schubert F, Seifert F, Elster C, Link A, Walzel M, Mientus S, Haas J, Rinneberg H. Serial 1H-MRS in relapsing-remitting multiple sclerosis: effects of interferon-beta therapy on absolute metabolite concentrations. MAGMA 2002;14:213–222.
9. Soher BJ, Young K, Maudsley AA. Representation of strong baseline contributions in 1H MR spectra. Magn Reson Med 2001;45: 966–972.
10. Weiland E, Roell S, Leibfritz D, Krueger G. Time-domain fitting of 1H-MR spectra of the human brain: a model-free integration of the macromolecular baseline. In: International Society for Magnetic Resonance in Medicine, Toronto, Canada; May, 2003. p 1160.
11. Young K, Soher BJ, Maudsley AA. Automated spectral analysis. II. Application of wavelet shrinkage for characterization of non-parameterized signals. Magn Reson Med 1998;40:816–821.
12. Cudalbu C, Mlynarik V, Xin L, Gruetter R. Quantification of in vivo short echo-time proton magnetic resonance spectra at 14.1 Tesla using two different approaches of modelling the macromolecule spectrum. Meas Sci Technol 2009;20:104034.
13. Hwang JH, Graham GD, Behar KL, Alger JR, Prichard JW, Rothman DL. Short echo time proton magnetic resonance spectroscopic imaging of macromolecule and metabolite signal intensities in the human brain. Magn Reson Med 1996;35:633–639.
14. Mlynarik V, Cudalbu C, Xin L, Gruetter R. 1H NMR spectroscopy of rat brain in vivo at 14.1Tesla: improvements in quantification of the neurochemical profile. J Magn Reson 2008;194:163–168.
15. Cavassila S, van Ormondt D, Graveron-Demilly D. Cramér-Rao bound analysis of spectroscopic signal processing methods. In: Yan H, editor. Signal processing for magnetic resonance imaging and spectroscopy, Vol. 22. New York: Marcel Dekker; 2002.
16. Coenradie Y, de Beer R, van Ormondt D, Cavassila S, Ratiney H, Graveron-Demilly D. Background-signal parametrization in in vivo MR spectroscopy. In Proceedings of ProRISC 2002;248–259.
17. Gottschalk M, Lamalle L, Segebarth C. Short-TE localised 1H MRS of the human brain at 3 T: quantification of the metabolite signals using two approaches to account for macromolecular signal contributions. NMR Biomed 2008;21:507–517.
18. Hofmann L, Slotboom J, Boesch C, Kreis R. Characterization of the macromolecule baseline in localized (1)H-MR spectra of human brain. Magn Reson Med 2001;46:855–863.
19. Stanley JA, Pettegrew JW. Postprocessing method to segregate and quantify the broad components underlying the phosphodiester spectral region of in vivo (31)P brain spectra. Magn Reson Med 2001;45: 390–396.
20. Hofmann L, Slotboom J, Jung B, Maloca P, Boesch C, Kreis R. Quantitative 1H-magnetic resonance spectroscopy of human brain: influence of composition and parameterization of the basis set in linear combination model-fitting. Magn Reson Med 2002;48:440–453.
21. Seeger U, Mader I, Nagele T, Grodd W, Lutz O, Klose U. Reliable detection of macromolecules in single-volume 1H NMR spectra of the human brain. Magn Reson Med 2001;45:948–954.
22. Pfeuffer J, Tkac I, Gruetter R. Extracellular-intracellular distribution of glucose and lactate in the rat brain assessed noninvasively by diffusion-weighted 1H nuclear magnetic resonance spectroscopy in vivo. J Cereb Blood Flow Metab 2000;20:736–746.
23. Mlynarik V, Gambarota G, Frenkel H, Gruetter R. Localized short-echo-time proton MR spectroscopy with full signal-intensity acquisition. Magn Reson Med 2006;56:965–970.
24. Mulkern R, Bowers J. Density matrix calculations of AB spectra from multipulse sequences: quantum mechanics meets in vivo specroscopy. Concepts Magn Reson 1994;6:1–23.
25. Govindaraju V, Young K, Maudsley AA. Proton NMR chemical shifts and coupling constants for brain metabolites. NMR Biomed 2000;13: 129–153.

26. Lei H, Zhang Y, Zhu XH, Chen W. Changes in the proton T2 relaxation times of cerebral water and metabolites during forebrain ischemia in rat at 9.4 T. Magn Reson Med 2003;49:979–984.
27. Xin L, Gambarota G, Mlynarik V, Gruetter R. Proton T2 relaxation time of J-coupled cerebral metabolites in rat brain at 9.4 T. NMR Biomed 2008;21:396–401.
28. Ellegood J, Hanstock CC, Beaulieu C. Diffusion tensor spectroscopy (DTS) of human brain. Magn Reson Med 2006;55:1–8.
29. de Graaf RA. In vivo NMR spectroscopy: principles and techniques. University of Virginia: Wiley; 1998; 269–277 p.
30. Cudalbu C, Mlynarik V, Xin L, Gruetter R. Comparison of T1 relaxation times of the neurochemical profile in rat brain at 9.4T and 14.1T. Magn Reson Med 2009;62:862–867.
31. de Graaf RA, Brown PB, McIntyre S, Nixon TW, Behar KL, Rothman DL. High magnetic field water and metabolite proton T1 and T2 relaxation in rat brain in vivo. Magn Reson Med 2006;56:386–394.
32. Pijnappel WWF, van den Boogaart A, de Beer R, van Ormondt D. SVD-based quantification of magnetic resonance signals. J Magn Reson 1992;97:122–134.